

Mechanical Properties and Durability of Concrete Containing Indonesian Coal Fly Ash

Fadhilah Muslim^{1,*}, Rachmat Hermawan^{2,3}

¹Department of Civil Engineering, Faculty of Engineering, Universitas Indonesia, Indonesia

²Department of Metallurgical and Material Engineering, Faculty of Engineering, Universitas Indonesia, Indonesia

³PT. PLN (Persero) Head Office, South Jakarta, Indonesia

Received July 21, 2024; Revised October 10, 2024; Accepted November 13, 2024

Cite This Paper in the Following Citation Styles

(a): [1] Fadhilah Muslim, Rachmat Hermawan, "Mechanical Properties and Durability of Concrete Containing Indonesian Coal Fly Ash," *Civil Engineering and Architecture*, Vol. 13, No. 1, pp. 331 - 348, 2025. DOI: 10.13189/cea.2025.130120.

(b): Fadhilah Muslim, Rachmat Hermawan (2025). *Mechanical Properties and Durability of Concrete Containing Indonesian Coal Fly Ash*. *Civil Engineering and Architecture*, 13(1), 331 - 348. DOI: 10.13189/cea.2025.130121.

Copyright©2025 by authors, all rights reserved. Authors agree that this article remains permanently open access under the terms of the Creative Commons Attribution License 4.0 International License

Abstract The use of cement, as the main construction material, is a major contributor to escalating global CO₂ emissions as cement production increases. To address this challenge and align with Sustainable Development Goals (SDGs), fly ash from boiler combustion has a potential to replace a partial percentage of cement as a waste material. In line with Indonesian Carbon neutral's strategy, biomass cofiring of Coal Fire Power Plant (CFPP) also contributes to net-balanced CO₂ emissions. This research explores the potential benefits of incorporating fly ash derived from coal and biomass co-firing at power plants on the properties of concrete. This paper presents a comprehensive investigation of the impact of co-firing on the mechanical properties and durability of concrete. Three concrete mixes prepared using Portland Cement CEM I and cement replacement by 10%, 20% and 30% fly ash (FA) were subjected to rigorous testing, including assessments of density, porosity, sorptivity, and electrochemical analysis. The results revealed that replacing 10% of cement with fly ash yielded the most optimal outcome, with the concrete exhibiting remarkable corrosion resistance. Specifically, it exhibited a density of 2.226 kg/m³, porosity of 26%, sorptivity of 0.3 mm/s^{0.5}, and a corrosion rate of 0.26 mm/year. Additionally, the Electrochemical Impedance Spectroscopy (EIS) test demonstrated enhanced corrosion resistance of the reinforcing steel across all variations of concrete specimens. This was further confirmed by the carbonation test, which indicated the absence of carbonation (indicated by pink areas). In conclusion, the utilization of fly ash

derived from coal and biomass co-firing in coal-fired power plants presents a promising alternative to traditional cement in concrete. This alternative material offers superior properties compared to concrete composed solely of Ordinary Portland Cement (OPC).

Keywords Fly Ash, Cofiring, Concrete, Mechanical Properties, Corrosion Resistance, Durability

1. Introduction

In terms of supporting the Sustainable Development Goals (SDGs) to accelerate the target of the new and renewable energy mix of 23% by 2025 [1], PT PLN (Persero), an electricity national company in Indonesia has conducted a strategic program CFPP. The fuel used is based on a mixture of biomass and coal which has the criteria of being easy, clean, sustainable, and based on people's economy. For this reason, Suralaya CFPP uses sawdust as a biomass base which is used with a mixture of 5% biomass and 95% coal.

In the process of burning coal, cofiring CFPP will produce fly ash which is classified as Fly Ash and Bottom Ash (FABA). FABA from the combustion process at CFPP is non-B3 waste according to government regulation number 22 of 2021 about the implementation of environmental protection and management [2]. Fly ash also could be utilized for construction raw materials such

as pozzolan on Pozzolan Portland Cement (PPC). In line with the US Environmental Protection Agency, 40 Code of Federal Regulations Parts 257 and 261 in 2015 issued arrangements for the disposal of coal combustion residues (FABA) as solid waste, not including the category of hazardous waste (B3 waste) [3].

Regarding environmental issues in encouraging global emission reduction, PPC cement production is declared to be more environmentally friendly than OPC cement which produces 5-10% of global carbon emissions [4]. PPC cement is produced with a mixture of 85-65% OPC cement and 15-40% pozzolan (fly ash or natural pozzolan) while the main composition of OPC cement is produced from clinker and calcium sulfate. Utilizing fly ash based on 95% of coal and 5% of saw dust as biomass in the OPC cement mixture, is expected to reduce the use of OPC and become a pozzolan material alternative for PPC cement.

The durability of concrete is the most important thing in showing reinforced concrete's performance in the structure's operating life. Chlorine-induced corrosion is an issue that is highly considered regarding these durability parameters. Concrete has an alkaline pH which helps in the passivation of reinforcing steel. While the entry of chloride ions causes depassivation and the concentration of chlorine ions will increase in the iron concrete [5].

Several previous researchers who studied the performance of reinforced concrete containing fly ash from low volumes of 10% - 30% were able to reduce the porosity concentration due to hydration reaction in the NaCl solution in which tricalcium aluminate (C3A) began to chemically bond with chlorine ions in the formation of Friedel's salt [6][7]. Another method studied by [8] with long-term curing also showed the result in reducing the chloride penetration coefficient.

The objective of this study is to determine the properties of concrete containing fly ash from Indonesian coal-fired power plant. The fly ash used comes from a mixture of coal 95% (a combination of low rank coal and medium rank coal) and 5% sawdust-based biomass at Suralaya CFPP Unit 8. There are potentially different material characteristics and corrosion rates that occur in the reinforcement concrete, while corrosion analysis used electrochemical impedance spectroscopy (EIS) and cyclic polarization test as well as proof of diffusion CO₂ which destroyed the passive layer of reinforcing steel using a carbonation test. With the above conditions, it is necessary to study the corrosion resistance of fly ash produced by the combustion of cofiring Suralaya CFPP Unit 8 based on sawdust 5% and 95% coal.

2. Materials and Methods

2.1. Materials and Mix Proportion

Three blended concrete mixes were prepared using Ordinary Portland Cement and cement replacement by 10%, 20% and 30% fly ash (ASTM C136, 2001) [9]. The chemical compositions of fly ash and cement were analyzed using x-ray fluorescence analysis (XRF) (model PANalytical Epsilon 1, serial DY:2416). The results are shown in Table 1.

Table 1. Chemical composition of Fly Ash and Cement

Element	Unit	Fly Ash	OPC	PPC
Al ₂ O ₃	%	13.73	1.91	4.00
SiO ₂	%	36.12	9.45	18.34
SO ₃	%	-	2.21	2.38
Cl	%	-	0.12	0.16
K ₂ O	%	0.86	0.57	1.28
CaO	%	19.81	80.25	66.55
TiO ₂	%	1.80	0.34	0.57
MnO	%	0.74	-	-
Fe ₂ O ₃	%	25.88	4.65	5.77
SrO	%	0.38	0.29	0.67
Ag ₂ O	%	0.43	0,22	0.27
BaO	%	0.25	-	-
Total	%	100	100	100

The low carbon steel was worn to be working electrode and the chemical composition of C 0.283 %wt, Si 0.166 %wt, Mn 0.415 %wt, P 0.029 %wt, S 0.03 %wt, Cr 0.373 %wt, Mo 0.013 %wt, and Ni 0.059 %wt. The dimensions of working electrode were Ø10 x 100 mm with both ends sealed by resin so that the length of the exposure surface was 60 mm and connected with cable in one end as shown in Figure 1.

2.2. Sample Preparation and Environmental Exposure

Referring to ASTM C192 [10], the concrete specimen used has dimensions of 100 x 200 mm with the mix design (MD) used in the study shown in Table 2. Water Cement ratio (W/C ratio) and Sand Aggregate ratio (S/A ratio) used in this study were 0.4 and 0.48 respectively. After being cured for 28 days, the specimens were tested for the mechanical properties.

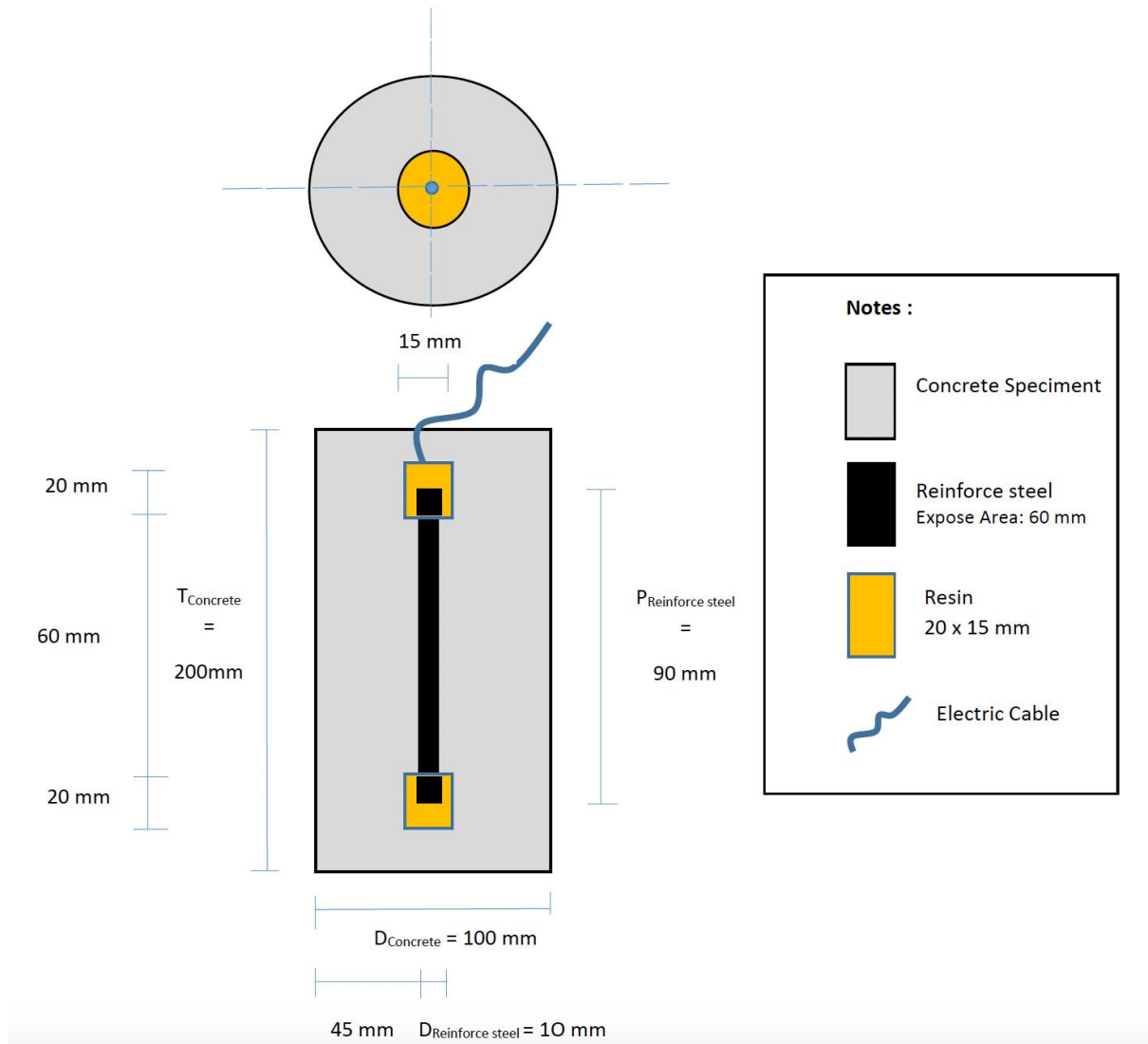


Figure 1. Mesh grid of topographic model

Table 2. Mix design of concrete specimen

Mix Design	Composition	W/C	S/A	Water [Kg]	Cement [Kg]	Sand [Kg]	Fly Ash [Kg]	Gravel [Kg]
MD-1	0FA100OPC	40%	47.9%	3.53	10.56	18.33	0	19.2
MD-2	0FA100PPC	40%	47.9%	3.53	10.56	18.33	0	19.2
MD-3	10FA90OPC	40%	47.9%	3.53	9.50	18.33	1.06	19.2
MD-4	20FA80OPC	40%	47.9%	3.53	8.44	18.33	2.11	19.2
MD-5	30FA70OPC	40%	47.9%	3.53	7.39	18.33	3.17	19.2

2.3. Compressive Strength Test

Compressive strength tests were carried out based on ASTM C39 [11] on concrete specimens aged 7 and 28 days using a digital compressive strength machine (Serial 2000.160120). Three specimens for each variation of mix design and curing period were tested.

2.4. Density and Void Test

Specific gravity and void content of concrete were evaluated using the ASTM C1754 [12] standard. In this test, 28 days concrete specimens were used with dimensions of 100 x 200 mm. The specimen was dried in an oven at a temperature of 105 ± 5 °C for 24 ± 1 hour and the weight of the specimen was weighed, then put it back in the oven for 2 hours and then measured the weight of the specimen. This method was repeated until a 0.5% difference in specimen weight was obtained. Next, the concrete specimen was soaked in water for 30 ± 3 minutes. Finally, the weight of the submerged concrete specimen was measured and the solid volume of the concrete specimen was determined. The void content was calculated using the difference between the total volume and the submerged volume.

2.5. Water Absorption Rate Test

The rate of water absorption in concrete specimens was tested by the ASTM C1585 [13] standard, and the test used 28-day-old specimens with dimensions of 100 ± 6 mm and length of 50 ± 3 mm. The specimens were dried in an oven at a temperature of 50 ± 2 °C for 3 days and then were stored in a sealed container for 15 days at a temperature of 23 ± 2 °C. The weight of samples was then measured. Prior to immersing the samples in water with a 1-3 mm depth from the submerged surface, the side of samples was covered using aluminium tape while the top of the specimen was covered with plastic. The weight of specimens was measured at intervals of 1, 5, 10, 20, 30, 60 etc. The rate of water absorption in concrete was calculated by determining the change in mass divided by the cross-sectional area of the specimen and the density of water.

2.6. Electrochemical Impedance Spectroscopy (EIS) Analysis

Concrete specimens with dimensions of 100 x 200 mm were prepared and immersed in the chloride environment with NaCl 3.5% with the measurement time variation at day-1, day-3, and day-6. The working electrode embedded in the concrete was low carbon steel with a reference electrode using silver-silver chloride and platinum used as a counter electrode. The test was carried out at room

temperature with a test frequency range of 10-2 to 105 Hz. EIS data and polarization analysis were carried out using FRA Impedance Potentiostatic (Model AUTOLAB PGSTAT302N serial AUT87891) with a potential range of Ecorr 1.5 V respectively.

2.7. Scanning Electron Microscope (SEM)

First, the concrete specimens were cut into a length of 5 mm, width of 5 mm, and thickness of 3 mm. Then the cut-specimens were coated using a carbon coating and followed by a vacuum process at a pressure of 5 – 5.9 mmHg. The last step was the process of observing the microstructure using SEM (model SEM Thermoscientific Quanta 650) to observe the air voids, crack width, and crack length in the concrete structure.

3. Results and Discussions

3.1. Microstructure of Fly Ash Concrete

The concrete specimens had a composition of the main raw materials namely cement, fly ash, coarse aggregate, sand, and water. Based on XRF analysis, the chemical composition of oxides possessed by fly ash, OPC cement, and PPC cement was observed. Refer to ASTM C618 [14] that the chemical composition of fly ash has the main composition, namely Al_2O_3 , SiO_2 , and Fe_2O_3 with a total percentage of 70% for class F. From the results of testing the chemical composition of fly ash used in this study according to Table 1 where the total composition was 75.73%, this indicates that the fly ash was classified as class F. The chemical content of fly ash greatly affects the hydration reaction process between fly ash, cement, and water. In the process, the water in the fresh concrete mixture will bind tricalcium silicate (C3S), which later becomes a calcium silicate hydrate gel ($3CaO \cdot 2SiO_2 \cdot 3H_2O$ or CSH) [15].

The spherical shape and particle size of fly ash can be seen from the results of the SEM test in Figure 2 while the particles of OPC cement are crystalline according to Figure 3. Research showed that pozzolanic material from fly ash can fill the Interface Transition Zone (ITZ) area due to the smaller particle size [16]. This is inversely proportional to the results of this study, and the results of the SEM test with a magnification of 500x and a scale of 20 μ m indicate that the fly ash particle size was larger than the cement particle size according to Figures 2-3. This is because the fly ash used is obtained from the area economizer hopper which has different characteristics of fly ash when obtained from the fly ash silo after passing through the electrostatic precipitator (ESP). This condition can have the impact of not filling the ITZ area of the concrete structure.

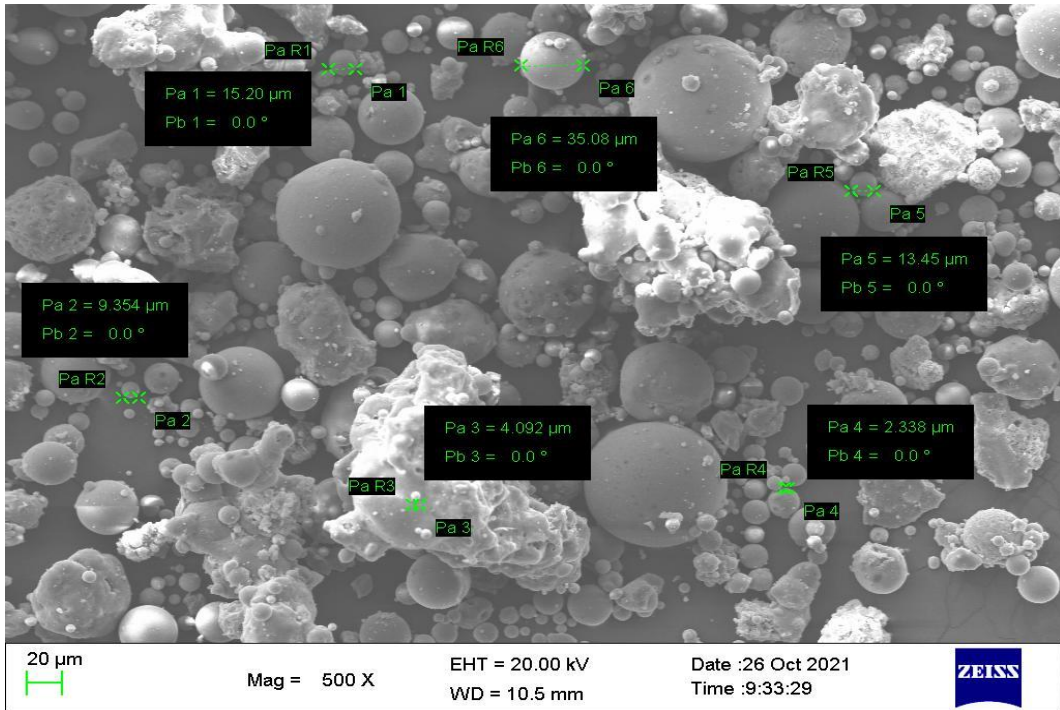


Figure 2. Microstructure of fly ash particle

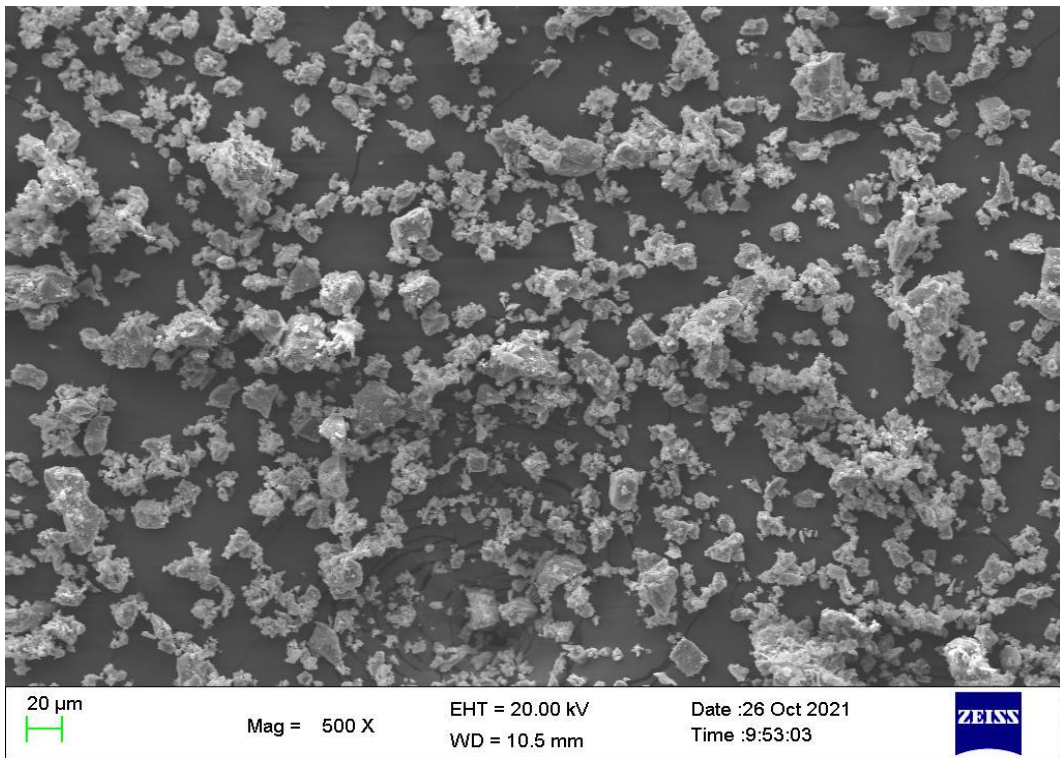


Figure 3. Microstructure of OPC particle

From the XRF analysis, it shows that fly ash is dominated by silica oxide (SiO_2) which will react with $\text{Ca}(\text{OH})_2$ released from the hydration process and will form CSH again or this ability is called self-healing capability [17]. $\text{Ca}(\text{OH})_2$ has weak characteristics that produce cavities or pores and contains micro cracks (microcrack) which will reduce the compressive strength of concrete. This re-formation of CSH will make the concrete denser so that the permeability will be smaller [18]. Other research [19] showed that the greater the percentage of fly ash mixture in cement, the higher the density, and the lower the porosity.

Concrete characteristics such as density, porosity, and sorptivity concrete determine the rate of diffusion of chloride and CO_2 on the environment NaCl. Along with the increase in density, the decrease in porosity and sorptivity can protect the passive layer on the reinforcing steel [18]. This is because in addition to density and porosity, what affects the rate of diffusion is water absorption or sorptivity.

However, in this study, it showed a decrease in density and an increase in porosity in the variation of concrete specimens containing fly ash compared to concrete specimens without fly ash according to Figures 4-5.

Related to the analysis of the quality of concrete, it was found that the composition of the 10FA90OPC concrete specimen against other variations of fly ash concrete specimens had a better-quality value of concrete where the results were 2225.81 kg/m^3 density, 25.91% porosity and sorptivity $0.323 \text{ mm/s}^{0.5}$. Looking at the results of the concrete quality test and corrosion resistance analysis in this study, it can be seen that 10FA90OPC was the most optimal composition of the fly ash and OPC cement

mixture where the density value was higher, and the porosity was lower than other fly ash mixtures 20FA80OPC and 30FA70OPC, with evidence from the results of the test sorptivity as the choice of the chloride ion penetration test method. In this study, it will affect the corrosion resistance where the corrosion rate value from the EIS and polarization test results was lower than 20FA80OPC and 30FA70OPC. Concrete characteristics such as density, porosity and sorptivity concrete determine the rate of diffusion of chloride and CO_2 on the environment NaCl. Along with the increase in density, the decrease in porosity and sorptivity can protect the passive layer on the reinforcing steel [18]. This is because in addition to density and porosity, what affects the rate of diffusion is water absorption or sorptivity.

Sorptivity shows the connectivity between cavities or pores in concrete. The results of sorptivity showed that the sorptivity in fly ash mixture was higher than in OPC cement or PPC cement. The test sorptivity shows that the sorptivity of concrete in specimens without fly ash was faster than concrete specimens with variations in fly ash mixture, resulting in faster initiation of corrosion [20]. This can be seen in Figure 6, each concrete specimen 10FA90OPC, 20FA80OPC, 30FA70OPC has a value of sorptivity 0.323, 0.423, and 0.471 ($\text{mm/s}^{0.5}$). Meanwhile, without fly ash mixture, the concrete specimens of 100 PPC and 100OPC were lower, namely 0.253 and 0.287 ($\text{mm/s}^{0.5}$). This phenomena is worsened by ITZ condition that contrary to other works [16] with adding more fly ash have performed on the ITZ. The higher mixture percentages 10%FA, 20%FA, 30%FA contribute higher porosity in ITZ caused by sizing of fly ash utilization so that the sorptivity would increase.

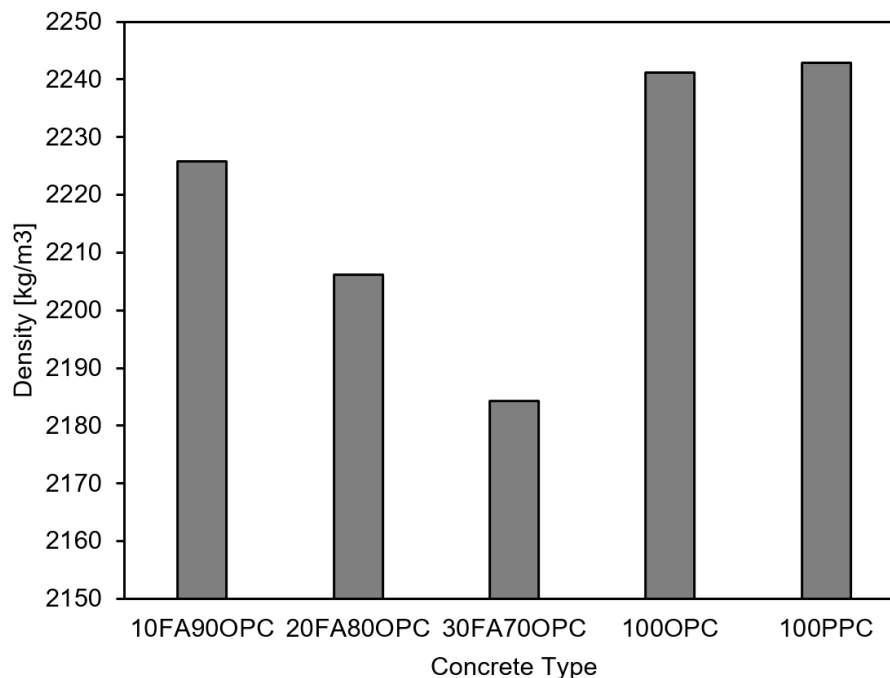


Figure 4. Effect of fly ash on the density of concrete specimens

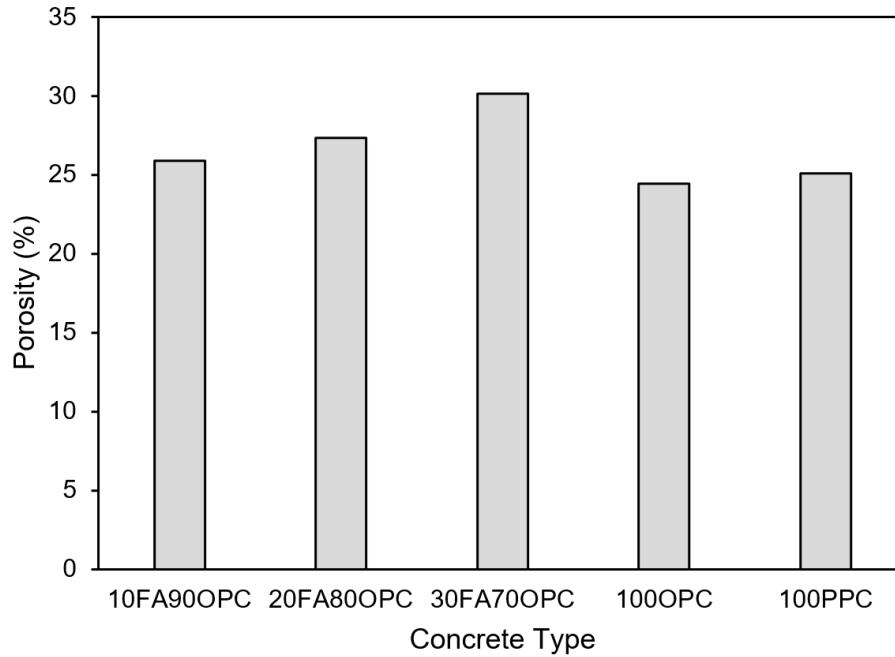


Figure 5. Effect of fly ash on the porosity of concrete specimens

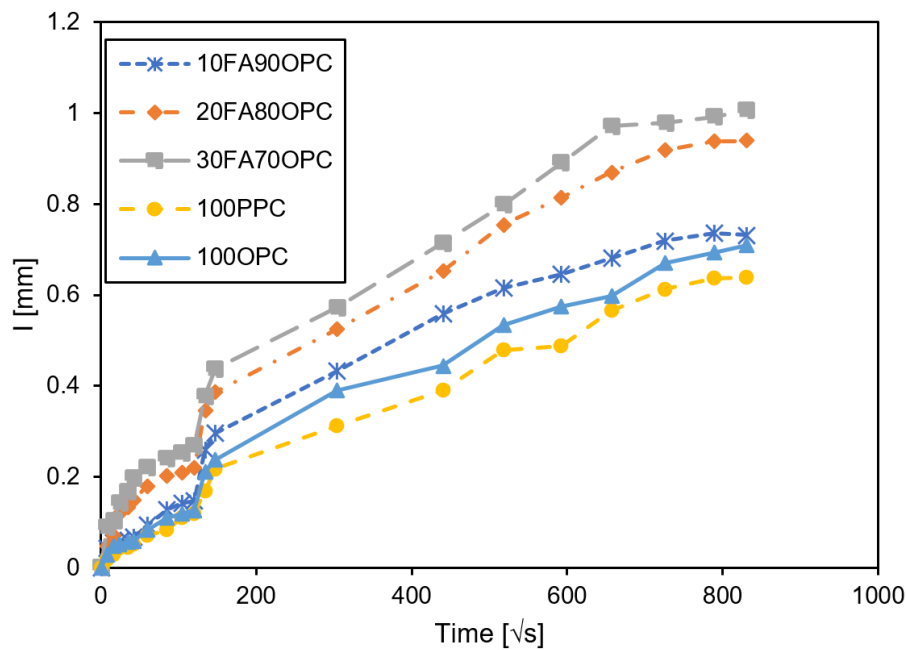


Figure 6. Effect of fly ash on sorptivity test result

3.2. Effect of Fly Ash on Compressive Strength

The values of density, porosity, and sorptivity affect the value of the compressive strength of concrete after the process of curing for 28 days which can be seen in Figure 7.

Based on the results of the compressive strength test as shown in Figure 7, concrete specimens containing no fly ash produced greater compressive strength compared to the specimens using fly ash. This is due to the hydration reaction between cement containing calcium silicate

elements with water progressing more quickly.

The slow process of the pozzolanic reaction [21] in fly ash concrete specimens is caused by the pozzolanic reaction which is influenced by the chemical reaction process between fly ash, water, and cement in the concrete. In the presence of pozzolanic elements in the concrete mixture, it will react with $\text{Ca}(\text{OH})_2$ to form a secondary reaction, namely calcium silicate hydrate again. The pozzolanic reaction is also determined by the amorphous of fly ash, where the more spherical fly ash particles, the

higher the amorphous degree of fly ash, and the more reactive the pozzolanic reaction [22]. With the increase of curing age to 28 days, there was an increase in the compressive strength even though the value of the compressive strength of fly ash concrete was slightly lower than without OPC cement fly ash. The compressive strength values for concrete specimens 10FA90OPC, 20FA80OPC, and 30FA70OPC were 32.9 MPa, 31.8 MPa, and 30.5 MPa respectively, which are lower than the concrete specimens of 100OPC and 100PPC, namely 33.6 MPa and 34.8 MPa. As the fly ash mixture increases, the compressive strength decreases.

This phenomenon was not only caused by the quality value of the concrete formed from the curing process for 28 days, it was also influenced by the characteristics of fly ash particles [18]. Other studies also show that fly ash had a lower fineness level than Portland cement so the concrete quality increases along with the increase of fly ash replacement to cement from 10 % up to 30% [23]. However, the replacement of cement with the fly ash of 40% and 50% would reduce the concrete strength. This condition is opposite to this study that 10% up to 30% lack condition of filling ITZ, which was due to the fly ash mixture having greater porosity and sorptivity as well as

lower density than concrete without fly ash mixture as shown in Figures 5- 6, resulting in a decrease in the compressive strength of fly ash. Based on Figure 7 the compressive strength of the fly ash concrete specimen has a value that was relatively the same as that of the concrete without fly ash, which indicates that the fly ash specimen can replace the use of OPC cement in the manufacture of concrete.

3.3. Correlation between Porosity and Transport

The general description of the Tafel polarization plot in Figure 8 showed that the concrete specimens incorporating fly ash display a shift in the value of E_{corr} and I_{corr} compared to those without fly ash. The shift of E_{corr} and I_{corr} between 10FA90OPC, 20FA80OPC, 30FA70OPC concrete specimens in the anode area is caused by the possibility of increasing the chloride ion concentration in the local solution around the surface of the reinforcing steel, increasing the surface area which is actively corroded or because of both. The increase in chloride ions was caused by the rate of diffusion [24] as evidenced by the results of the sorptivity on concrete in Figure 6.

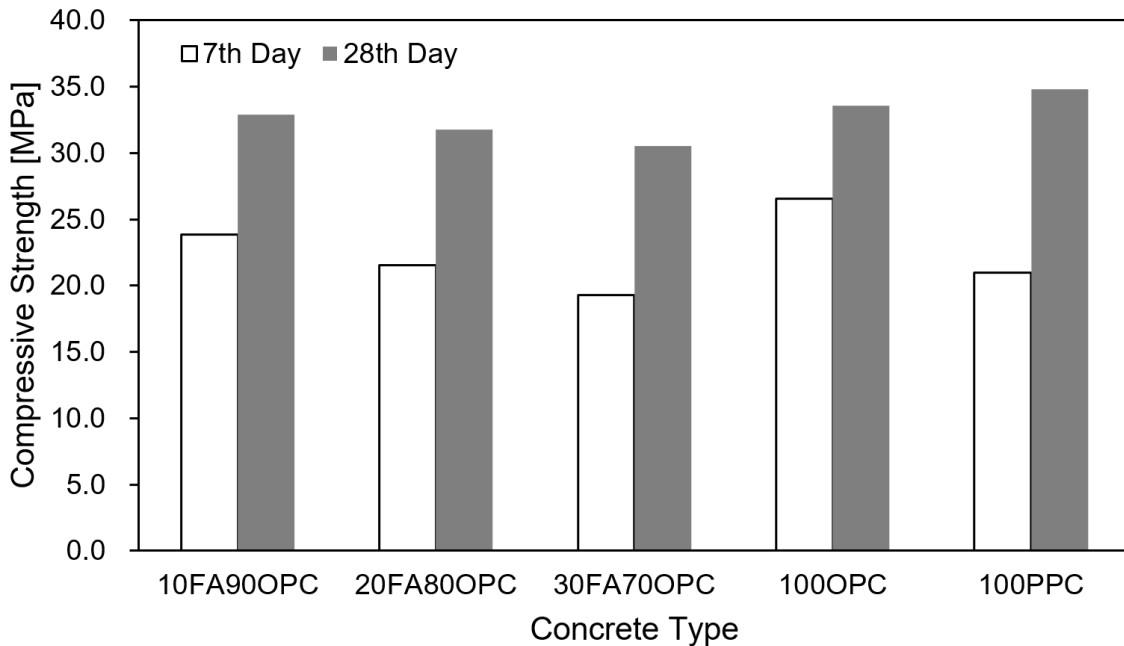


Figure 7. Effect of fly ash on compressive strength at curing ages of 7th Day and 28th Day

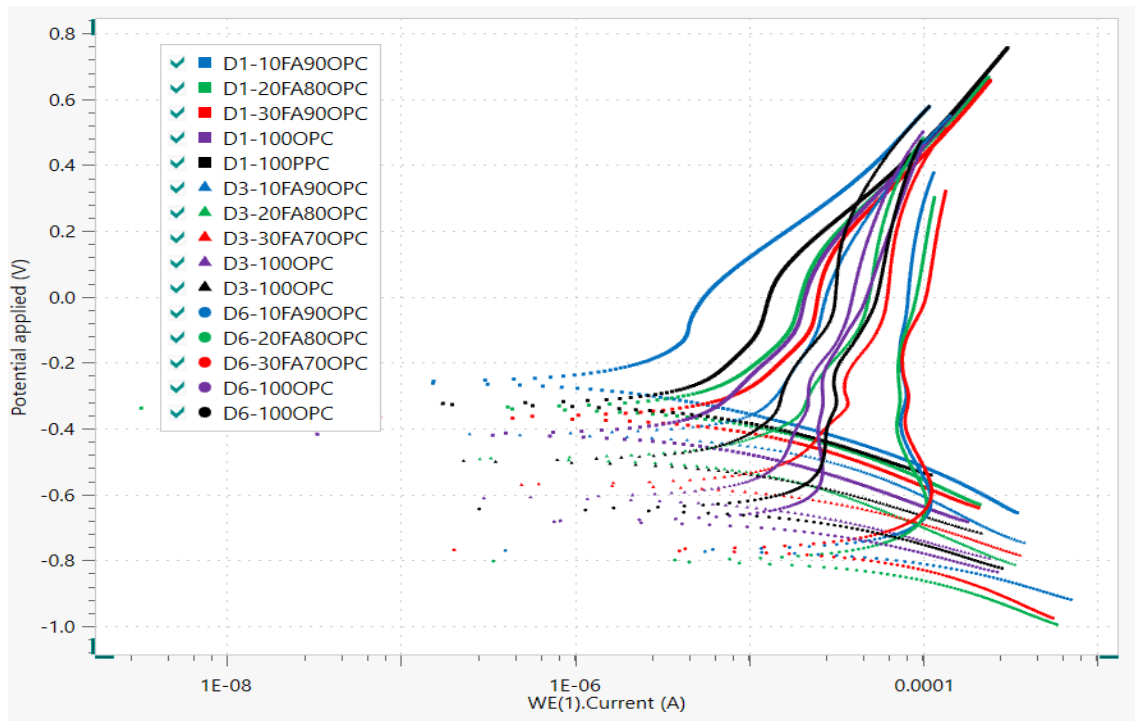


Figure 8. Linear Polarization Tafel plot concrete specimens vs SCE

In Tables 3-5, the polarization of concrete specimens on day 1 to day 6 shows that concrete specimens without fly ash 100PPC had the best value compared to other variations of concrete specimens in corrosion resistance, which obtained E_{corr} in the range of -325.48 mV to become -645.28 mV and the value of I_{corr} has a range of 1.52 to 27.10 μA . When compared with the variation of concrete specimens with fly ash, it shows that the 10FA90OPC concrete specimen had more stable corrosion kinetics than the 20FA80OPC and 30FA70OPC specimens, where E_{corr} and I_{corr} display a not too large deviation value from day 1 to day 6, the value of E_{corr} in the range of -259.44 mV to -768.73 mV and the value of I_{corr} has a range of 1.09 to 38.25 μA . For the 20FA80OPC specimen, the E_{corr} ranged from -337.96 mV to -802.66 mV and the I_{corr} ranged from 1.13 to 41.04 μA . while the 30FA70OPC concrete specimen obtained E_{corr} in the range of -366.24 mV to -870.62 mV and the value of I_{corr} has a range of 1.92 to 46.06 μA . The Tafel plot also shows the passivation area with a greater range in the anode area for fly ash concrete, and the passivation area also tends to be stable. The passivation mechanism in concrete with the fly ash mixture was also seen in previous studies [25].

Based on the value of E_{corr} from the Tafel Polarization plot, the average value is less than -350mV, except for the concrete samples of 10FA90OPC, 20FA80OPC and 100PPC by immersion on day 1. The value of $E_{\text{corr}} < -350$ mV indicates that there is a greater than 90% possibility of corrosion of reinforcing steel in the area at the time of measurement, while the value of $-350 \text{ mV} \leq E_{\text{corr}} \leq -200$ mV indicates that the corrosion activity of reinforcing

steel in the area is uncertain, or the probability of corrosion is 50% [26].

The results of measurements of the corrosion rate of reinforcing steel on day 1 to day 6 for 100PPC concrete specimens were in the range of 0.00945 to 0.16845 mm/year with the lowest corrosion rate, then 100OPC 0.00939 to 0.18440 mm/year, then 10FA90OPC concrete specimens with a value of 0.00130 to 0.25509 mm/year, followed by 20FA80OPC concrete specimens 0.00701 to 0.34495 mm/year, and 30FA70OPC concrete specimens 0.01191 to 0.35769 mm/year. Based on the value of corrosion rate from Tables 3-4, the plot on the Polarization Tafel shows the corrosion rate of reinforcing steel for concrete with and without fly ash in the excellent (very good) because it has a corrosion rate of 0.02 to 0.1 mm/year which occurs on the 1st and 3rd days. Meanwhile, the corrosion rate on the 6th day varies greatly because it depends on sorptivity, density and porosity. The corrosion rate value for the 10FA90OPC concrete specimen is in the range of 0.00130 to 0.25509 mm/year, and the corrosion rate value was in the excellent (very good) and good (good) categories. It can be concluded that the chloride ion content and exposure time greatly influence the corrosion behavior of reinforcing steel.

In addition, from the analysis of corrosion resistance through the Polarization Tafel method, the Tafel plot also shows the passivation area with a larger range in the anode area for concrete with fly ash, and the passivation area also tends to be stable. The passivation mechanism in concrete with the fly ash mixture was also seen in previous studies

[25]. The Polarization Tafel plot informs that the 10FA90OPC concrete specimen has the lowest corrosion rate compared to other variations of fly ash mixture of 0.25509 mm/year although it is higher than PPC cement at 0.16845 mm/year. It can be concluded that the chloride ion content and exposure time are very influential on the corrosion behavior of reinforcing steel.

Figure 9 shows the ability of the corrosion resistance of concrete specimens varies which is strongly influenced by the time immersion. The results bode plot and bode phase as shown in Figures 10(a)-(b) that in the low frequency range of 0.01 to 1 Hz impedance value shifted from area to area resistive capacitive, this indicates the presence of a highly resistive passive layer on the surface of the reinforcing steel due to the high pH of the concrete [27]. In addition, the impedance at low frequencies is also affected by electroactive diffusion by oxygen, the effect of layers of iron oxide, hydroxyl, and chloride ions through the oxide

layer to the electrode (reinforcement steel) and coupled with the charge transfer reaction [28]. The lowest impedance value by immersion on the 1st day is 353.405 Ω which occurs in the 30FA70OPC concrete specimen with a passage angle of 30.201°, for the highest impedance value 11467,287 Ω occurs in the 10FA90OPC concrete specimen with a passage angle of 72.515°. Meanwhile, for concrete specimens immersed on the 3rd day, the lowest impedance value is 344.438 Ω which occurs in the 30FA70OPC specimen with a fitting angle of 27.442°. The highest impedance value is 10413,872 Ω on 100PPC concrete specimens with a fitting angle of 59,588°. For concrete specimens immersed on the 6th day, the lowest impedance value is 288.773 Ω , which occurs in the 30FA70OPC specimen with a fitting angle of 18.712°. The highest impedance value is 8673,973 on 100PPC concrete specimens with an angle of 61,104°.

Table 3. Polarization Tafel for the 1st day concrete specimens

Concrete	Ecorr.Calc [mV]	Ecorr.Obs [mV]	Icorr [μ A]	Rpol [k Ω]	Corr rate [mm/yr]
10FA90OPC	-259,42	-259,44	1,09	9,427	0,00130
20FA80OPC	-338,82	-337,96	1,13	8,654	0,00701
30FA70OPC	-366,09	-366,24	1,92	6,002	0,01191
100OPC	-414,92	-417,66	1,51	8,293	0,00939
100PPC	-325,06	-325,84	1,52	8,279	0,00945

Table 4. Polarization Tafel for the 3rd day concrete specimens

Concrete	Ecorr.Calc [mV]	Ecorr.Obs [mV]	Icorr [μ A]	Rpol [k Ω]	Corr rate [mm/yr]
10FA90OPC	-413,84	-418,67	2,44	4,231	0,01879
20FA80OPC	-491,32	-492,21	2,84	3,346	0,02143
30FA70OPC	-566,98	-570,54	3,16	2,738	0,03568
100OPC	-609,56	-610,81	2,25	4,894	0,01648
100PPC	-498,52	-499,71	1,59	5,214	0,00991

Table 5. Polarization Tafel for the 6th day concrete specimens

Concrete	Ecorr.Calc [mV]	Ecorr.Obs [mV]	Icorr [μ A]	Rpol [k Ω]	Corr rate [mm/yr]
10FA90OPC	-768,27	-768,73	38,25	0,738	0,25509
20FA80OPC	-801,64	-802,66	41,04	0,736	0,34495
30FA70OPC	-868,89	-870,62	46,06	0,516	0,35769
100OPC	-682,72	-682,13	29,67	1,925	0,18440
100PPC	-643,97	-645,28	27,10	2,135	0,16845

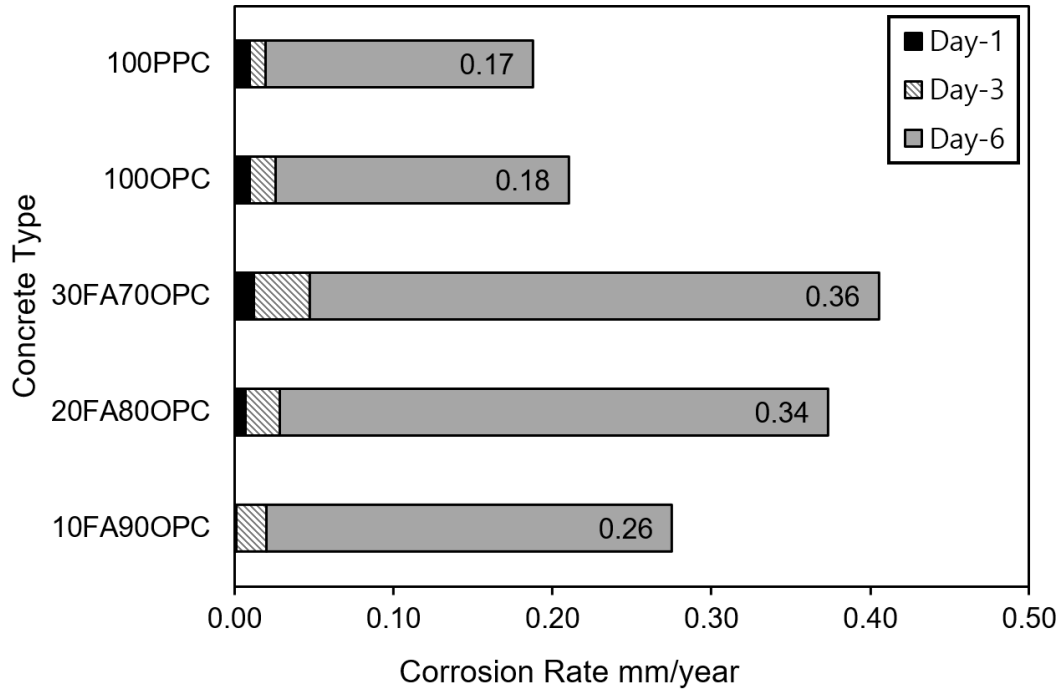
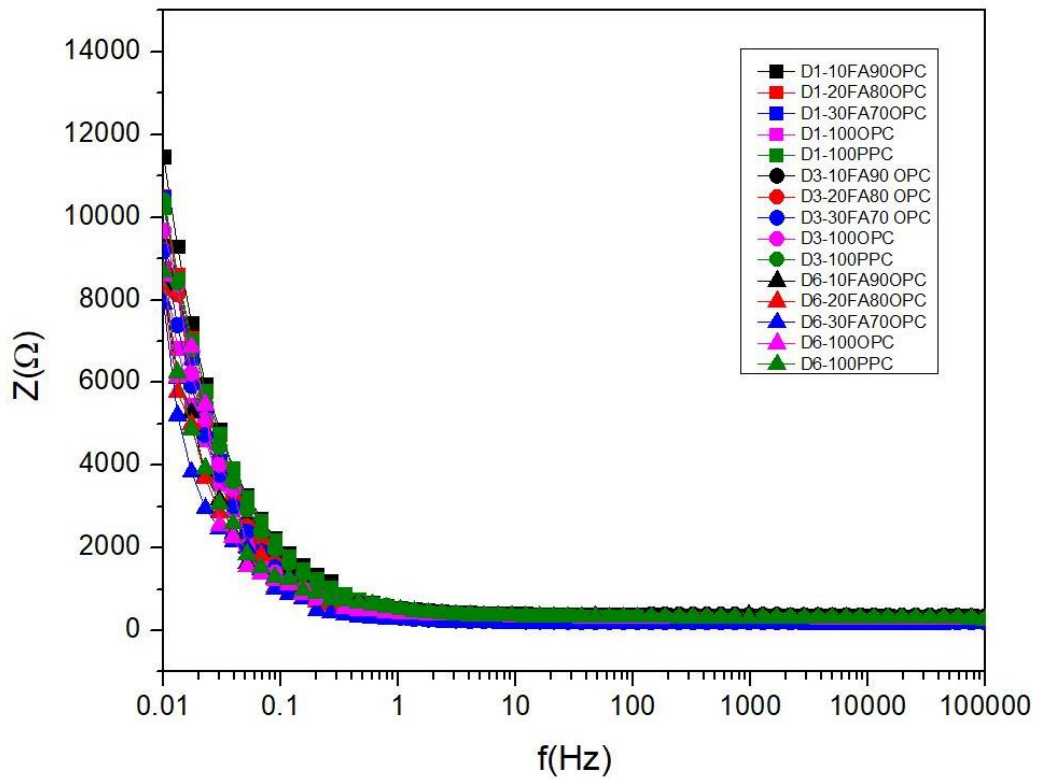
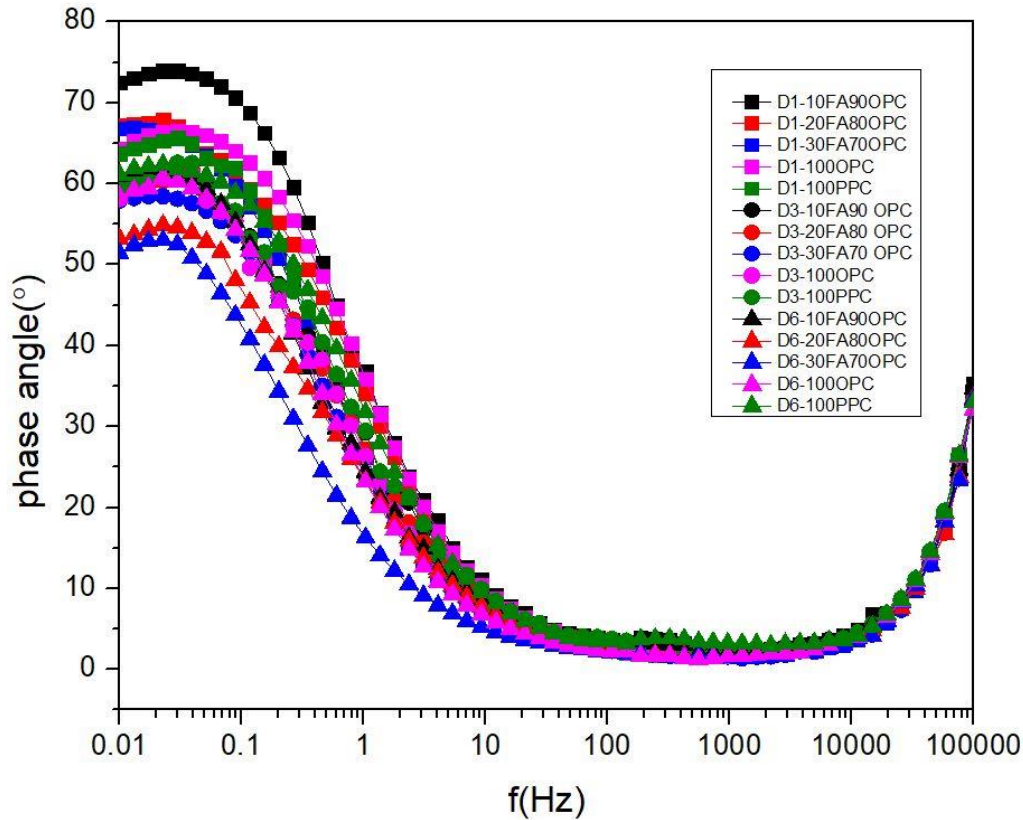


Figure 9. Graphic corrosion rate in each concrete specimen with immerse time function



(a)



(b)

Figure 10. (a) Fitting Bode Plot Electrochemical Impedance Spectroscopy (EIS) results of concrete specimens; (b) Fitting Bode Phase Electrochemical Impedance Spectroscopy (EIS) results of concrete specimens

In the medium frequency range of 1 Hz to 100 Hz, the impedance value is still shifting from the resistive to the capacitive area, but the change in the impedance value looks smaller and more stable. This phenomenon represents the resistance and capacitance of the concrete microstructure and the reinforcing steel interface area [29], where the impedance generated by the constant phase element bulk concrete will affect the faraday at the interface of the passive layer and reinforcing steel, and this resistance arises due to the charge transfer process with corrosion products on the surface. [30]. The lowest impedance value from the fitting of 1 to 100 Hz for concrete specimens by immersing on the 1st day is 220.079 Ω occurred in the 30FA70OPC concrete specimen with a passage angle of 2.734°, for the highest impedance value it is 561.982 Ω that occurs in concrete specimens 10FA90OPC with 29,276°. Meanwhile, for concrete specimens immersed on the 3rd day, the lowest impedance value is 207.134 Ω which occurs in the 30FA70OPC specimen with an angle of 2.687°, for the highest impedance value it is 511.090 Ω in the 100PPC concrete specimen with a fitting angle of 29.431°. For concrete specimens immersed on the 6th day, the lowest impedance value is 209.579 Ω which occurs in the 30FA70OPC specimen with a fitting angle of 2.259°. The highest impedance value is 508,544 Ω on 100PPC concrete

specimens with a fitting angle of 31,763°. The phenomenon from the results of Bode phase fittings, where the change in the phase angle formed between Z_{real} dan $Z_{imaginer}$ about the Z_{real} axis is not significant either on concrete specimens with the addition of fly ash or without the addition of fly ash.

Impedance spectra Bode plot and Bode phase in the high frequency range of 100 to 100 kHz show results that tend to be constant with phase angles close to 0° and experience a slight increase at frequencies close to 1 kHz. This phenomenon occurred in all specimens using fly ash or without using fly ash. The resistive behavior shown in the frequency range of 100 to 100 kHz is used as the basis for determining high frequencies in concrete specimens, because the impedance modulus provides an accurate estimate of the concrete resistance.

This phenomenon also shows that the low frequency range has a larger phase angle than the high frequency. This phase angle shift is related to the passive layer resistance, faraday process and capacitance double layer on the reinforcing steel surface [29].

In evaluating the results of the EIS test on reinforced concrete with variations in the mixture of fly ash in a chloride environment, modeling can be carried out using the Equivalent Circuit (EC). There are two EC models used, namely Figure 11(a) EC for specimens without fly ash and

Figure 11(b) EC for specimens using a mixture of fly ash. The selection of this EC model was based on the characteristics of the EIS spectrum obtained from the test results and was determined by the corrosion process on the surface and the condition of the reinforced concrete surface carried out by previous studies [26].

R_s in EC model was used to show resistance of 3.5% NaCl solution. CPE_1 and R_1 were used to show the constant phase element and the resistance of the concrete layer during the reaction, while CPE_2 and R_2 were used to show the constant phase element and the resistance of the concrete at the interface area of the reinforcing steel with

the concrete. The compounds involved include calcium hydroxide ($Ca(OH)_2$), tricalcium aluminate ($3CaO \cdot Al_2O_3$) and tetra calcium ferrite aluminate ($4CaO \cdot Al_2O_3 \cdot Fe_2O_3$). CPE_{dl} and R_{ct} are used to show the double layer resistance charge transfer on the reinforcing steel surface during the electrochemical process.

The impedance parameter values obtained from the model EC fittings are shown in Tables 6-8. In this study, the corrosion rate is influenced by several main parameters, namely the composition of fly ash to OPC cement, variations in time, and environmental conditions of chloride.

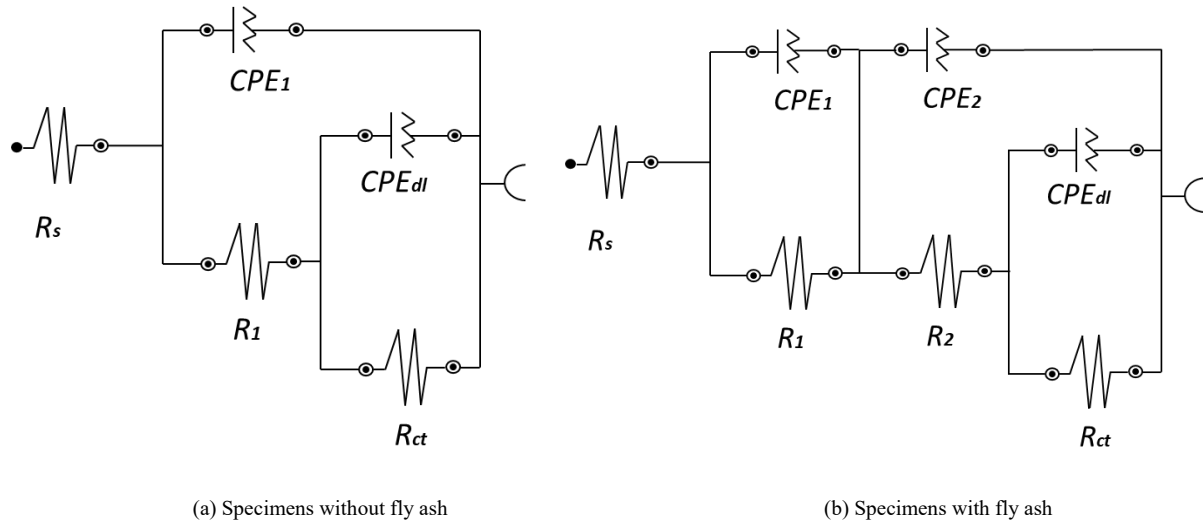


Figure 11. Equivalent Circuit (EC) model

Table 6. The results of the EIS fitting for the 1st day concrete specimens

Concrete	R_s [Ω]	CPE_1 [μF]			CPE_2 [μF]			CPE_{dl} [μF]		R_{ct} [Ω]
		Y_0 [μMho]	N	R_1 [Ω]	Y_0 [μMho]	N	R_2 [Ω]	Y_0 [μMho]	N	
10FA90OPC	362.21	552	0.782	182.32	0.00285	0.872	351.61	0.00281	0.972	1.1E+12
20FA80OPC	358.68	661	0.745	166.28	0.00363	0.701	253.56	0.00325	0.794	1.1E+12
30FA70OPC	251.46	950	0.865	114.90	0.00801	0.761	211.84	0.00763	0.615	1.1E+12
100OPC	352.32	695	0.874	81.04	N/A	N/A	N/A	4.41	0.745	1.1E+12
100PPC	347.81	767	0.885	82.83	N/A	N/A	N/A	3.82	0.794	1.1E+12

Table 7. The results of the EIS fitting for the 3rd day concrete specimens

Concrete	R_s [Ω]	CPE_1 [μF]			CPE_2 [μF]			R_2 [Ω]	CPE_{dl} [μF]		R_{ct} [Ω]
		Y_0 [μMho]	N	R_1 [Ω]	Y_0 [μMho]	N	Y_0 [μMho]		N		
10FA90OPC	304.55	1210	0.718	147.22	0.00338	0.941	333.18	0.00353	0.942	1.1E+12	
20FA80OPC	262.77	1380	0.712	132.49	0.00428	0.821	232.42	0.00747	0.758	1.1E+12	
30FA70OPC	231.93	1410	0.846	102.33	0.00993	0.972	177.71	0.00799	0.834	1.1E+12	
100OPC	323.479	910	0.818	53.12	N/A	N/A	N/A	3.05	0.731	1.1E+12	
100PPC	338,202	882	0,795	56,03	N/A	N/A	N/A	2,15	0,734	1.1E+12	

Table 8. The results of the EIS fitting for the 6th day concrete specimens

Concrete	Rs [Ω]	CPE ₁ [μF]			CPE ₂ [μF]			CPE _{ct} [μF]		R _{ct} [Ω]
		Y0 [μMho]	N	R1 [Ω]	Y0 [μMho]	N	R2 [Ω]	Y0 [μMho]	N	
10FA90OPC	213.12	1690	0.655	136.50	0.00452	0.473	286.32	0.00684	0.482	1.1E+12
20FA80OPC	190.56	1910	0.636	128.35	0.00675	0.775	210.33	0.00782	0.615	1.1E+12
30FA70OPC	164.01	2150	0.767	97.35	0.01146	0.832	165.19	0.00835	0.799	1.1E+12
100OPC	232.88	1582	0.795	48.90	N/A	N/A	N/A	6.44	0.732	1.1E+12
100PPC	294.86	1365	0.797	51.64	N/A	N/A	N/A	6.13	0.729	1.1E+12

This main parameter data was obtained from solution resistance (R_s) of concrete specimens in the range of 132.88 to 352.21 Ω, where the resistance decreases with time immersed in 3.5% NaCl until the 6th day. The solution resistance value (R_s) decreased with increasing electrolyte content in the concrete pores and the humidity of the concrete layer, which was due to the sorptivity which represented the chloride ion penetration rate.

This research shows that 10FA90OPC concrete has greater solution resistance (R_s) than 100PPC or 100OPC concrete specimens, although the sorptivity appears to be greater. This is because the pozzolanic reaction is also determined by the amorphous of fly ash [31], where the more spherical fly ash particles, the higher the amorphous fly ash and the more reactive the pozzolanic reaction. But in the 30FA70OPC concrete composition, the lowest value of R_s is strongly influenced by the values of density, porosity, and sorptivity.

From Table 8 the results of the EIS fitting for the 6th day concrete specimen, it can be seen that the R_1 of the 100PPC concrete specimen on the 6th day has a smaller value than concrete with a mixture of fly ash and OPC cement. The high resistance value corresponds to the passive state of reinforcing steel in the concrete due to the formation of a passive layer during the curing in addition to the SiO_2 and Al_2O_3 content fly ash in forming complex organic compounds (gel compounds) which limit the penetration of chloride ions leading to a porosity blocking effect on cement [18], so that the 10FA90OPC concrete specimen has an R value of 182.32 Ω, 147.22 Ω and 136.50 Ω for the measurement time during immersion on the 1st, 3rd, and 6th days. The decrease in the value of R_1 occurs due to layer damage passively on the surface of reinforcing steel due to the initiation of corrosion caused by chloride ions. The condition of the concrete structure which has a sorptivity can facilitate the penetration of chloride ions into the concrete structure so as to accelerate the corrosion process on the surface of the reinforcing steel [32]. The decrease in the value of R_1 for each concrete specimen was

also followed by an increase in the value of CPE_1 of concrete. This phenomenon was related to the non-uniformity of pitting and the heterogeneity of corrosion products on the surface of the reinforcing steel which was determined by the resistance ability of each concrete specimen.

The fitting found that the R_{ct} is very high, namely 1.1E+12 Ω, R_{ct} in general can be caused by the formation of a passive layer of Fe_3O_4 or Fe_2O_3 and or $\gamma\text{-FeOOH}$ on the surface of the reinforcing steel due to the high alkali content and (pH 12-13) in all reinforced concrete specimens. The formation of the above passive layer follows the electrochemical reaction in Eqs (1)-(3) [33].



All variations of concrete specimens with or without the addition of fly ash had a high R_{ct} value for all variations of the immersion. This shows that the addition of fly ash has an impact on the magnitude of the concrete resistance and the formation of a passive layer of reinforcing steel as evidenced from the results of the fitting bode plot in Figure 11. Meanwhile, the phenomenon of R_s , R_1 , R_2 decreased, because the function of exposure to chloride ions increased.

This phenomenon can explain that the passive layer on the surface of the reinforcing steel will remain intact which was indicated by R_{ct} value of 1.1E+12 Ω in all specimens and was evidenced by the results of the carbonation test indicated in pink in Figure 12. This shows that each specimen has not had a carbonation process in all of the reinforced concrete specimens. In other words, in the carbonation test, the absence of carbonation, typically indicated by pink areas when using phenolphthalein as an indicator, suggests that the concrete with fly ash exhibits superior resistance to carbonation. This lack of carbonation can be attributed to several factors related to the incorporation of fly ash.

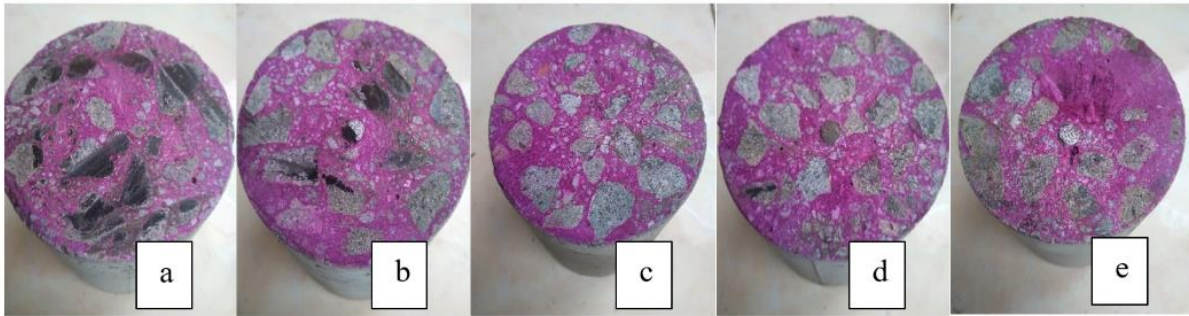


Figure 12. Carbonation test a) 10FA90OPC; b) 20FA80OPC; c) 30FA70OPC; d) 100OPC; e) 100PPC

On the other hand, an increase in chloride ion concentration which was confirmed by an increase in sorptivity also had an impact on an increase in the value of Y_0 CPE_{dl} for each time, namely on the 1st, 3rd and 6th days for each specimen from 0.00281 to 6.44 Mho.

Fittings of CPE₂ show the contribution of fly ash impedance to the 10FA90OPC, 20FA80OPC, and 30FA70OPC concrete specimens. The value of N (capacitance level) indicates the degree of deviation of the actual capacitance to ideal conditions. The presence of fly ash was thought to increase the passive behavior and increase the corrosion resistance of reinforcing steel in concrete [34].

Referring to Tables 6-8 regarding the relationship between concrete resistance and the possibility of corrosion, all specimens having an $R_{ct} > 20 \text{ k}\Omega\cdot\text{cm}^2$ have a low corrosion probability category [35]. It can be concluded that the resistance of concrete is strongly influenced by the composition of the concrete to cement, exposure time and chloride environment, because the higher the rate of diffusion of chloride ions into the concrete structure, the higher the concentration of chloride ions in the concrete structure so that it will reduce the resistance of the concrete, damaging the passive layer reinforcing steel in concrete and accelerating the corrosion of reinforcing steel.

Based on discussion above, it can be concluded that high fly ash content (30% fly ash) has a lower corrosion resistance than low fly ash concrete (10% fly ash) to reinforce steel as illustrated diagram in Figure 13. The presence of fly ash from biomass co-firing, due to its higher silica content, lower carbon and heavy metal content, reduces the permeability of the concrete and increases its density, making it more difficult for aggressive substances like chlorides to penetrate and reach the reinforcing steel that has been analyzed with Tafel polarization and Electrochemical Impedance Spectroscopy (EIS) method on sub chapter 3.3. 10% fly ash content helps create a denser caused of lower porosity, lower sorptivity and more uniform microstructure, minimizing the pathways for the movement of moisture and chloride ion induced. The reduced permeability and improved microstructure contribute to a higher resistance to corrosion and enhance the durability of the reinforced concrete. The incorporation

of 10% fly ash in concrete significantly improves corrosion resistance compared to other percentages, as evidenced by Electrochemical Impedance Spectroscopy (EIS) and carbonation test results. This specific dosage strikes a balance, enhancing the microstructural integrity of the concrete without compromising its workability. EIS tests reveal that concrete with 10% fly ash exhibits a marked increase in impedance, indicating reduced ionic conductivity and enhanced resistance to charge transfer processes, which are critical for mitigating corrosion. This improvement is attributed to the formation of a denser microstructure that limits the ingress of aggressive ions, such as chlorides.

Moreover, the carbonation tests show less carbonation penetration in concrete with 10% fly ash, evidenced by a reduced area of pink coloration, which signifies lower levels of carbon dioxide infiltration. This reduction is crucial as it decreases the potential for the formation of acidic conditions that can accelerate corrosion of the embedded steel reinforcement. In contrast, higher or lower percentages of fly ash do not yield the same level of enhancement in corrosion resistance, as they may lead to either insufficient pozzolanic activity or excessive dilution of the cement matrix. Thus, the 10% fly ash blend optimally balances performance and durability, significantly enhancing the corrosion resistance of concrete in aggressive environments. In other cases, 30% fly ash content has more pore and lower mechanical properties because the fly ash used is obtained from the area economizer hopper which has different characteristics of fly ash when obtained from the fly ash silo after passing through the electrostatic precipitator (ESP). This condition can have the impact of not filling the ITZ area of the concrete structure.

Figure 14 shows an increase in the pH of the solution which was caused by the degree of ionization. The ions are adsorbed onto the surface of the concrete specimen which acts as an anode reaction inhibitor, thus helping in slowing down the corrosion rate. But as the time increases immersion, the values of sorptivity and porosity are related to each other so that the aggressive ions can penetrate the pores so that it can accelerate the destruction of the passive layer on the reinforcing steel.

Further work is needed to test different percentages and

types of Fly Ash from different coal fire power plants in Indonesia used in concrete to establish their impact on long-term performance of concrete containing fly-ash from biomass co-firing. It is also important to test different durability properties including oxygen diffusivity, oxygen permeability, electrical conductivity, carbonation and chloride-induced corrosion, after being exposed to different environmental conditions for a longer duration. It is worth noting that the incorporation of fly ash in concrete production supports Indonesia's carbon neutrality goals by reducing the reliance on OPC, which is highly carbon intensive. By substituting cement with fly ash, the

construction industry lowers CO₂ emissions, conserves energy, and utilizes waste from power generation, aligning with Sustainable Development Goals (SDGs) like SDG 12 (Responsible Consumption and Production) and SDG 13 (Climate Action). This also promotes a circular economy, minimizes industrial waste, and reduces the environmental burden on landfills. Implementing biomass fly ash on a large scale requires the development of standardized testing and regulations to ensure consistent performance and compatibility with existing concrete production processes.

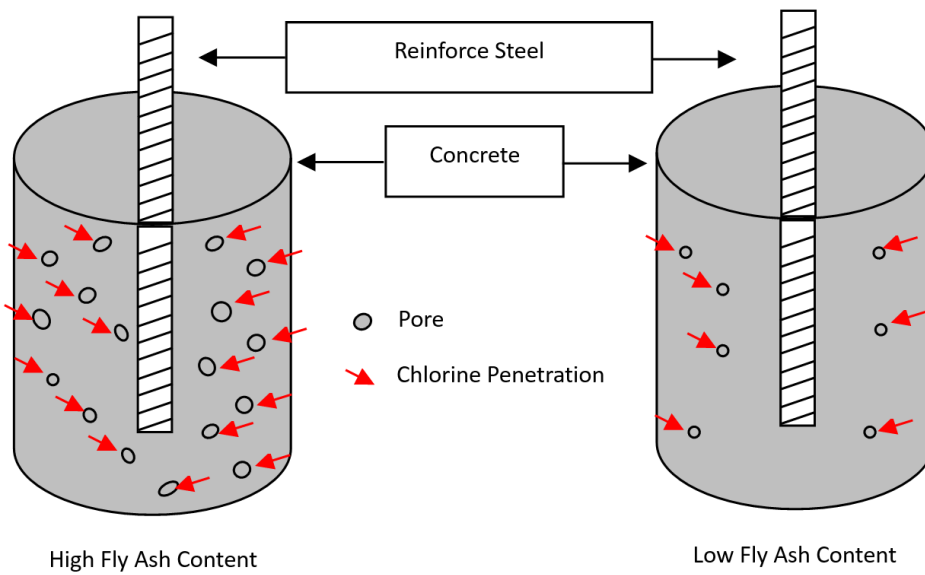


Figure 13. Comparison diagram of high and low fly ash content contributes to corrosion resistance

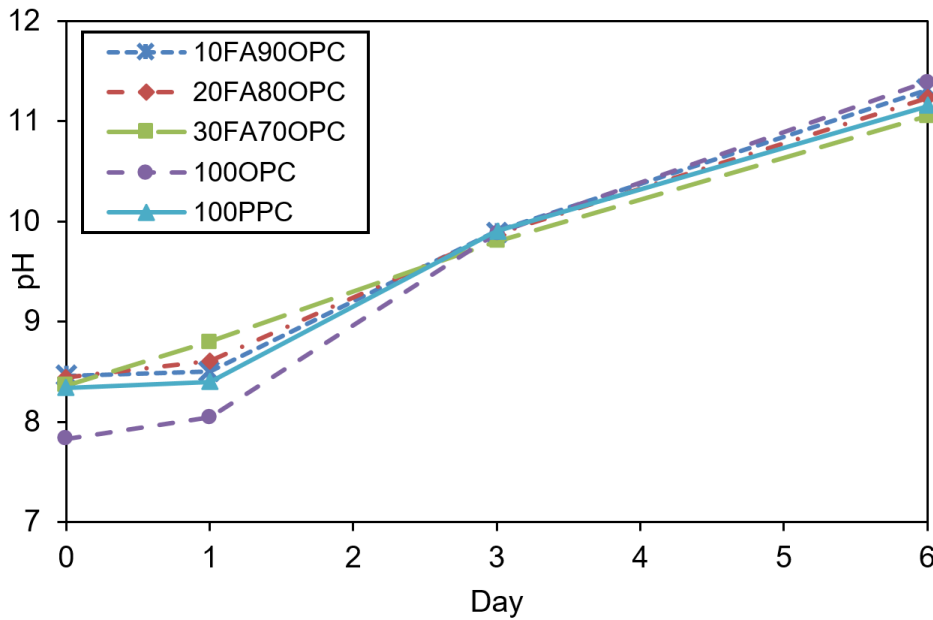


Figure 14. Graphic correlation pH solution to immerse time function

4. Conclusions

Based on the research conducted, several results were obtained related to the relationship between the chemical composition of concrete, the microstructure of fly ash particles, and the results of the quality test of concrete on the corrosion resistance of concrete reinforcing steel immersed in a 3.5% NaCl solution with variations in measurement time up to the 6th day. The conclusions obtained in this study are described as follows:

1. The properties of concrete specimens containing fly ash namely density, porosity, sorptivity, and compressive strength at the curing age of 28d had relatively the same values as concrete specimens without fly ash.
2. The concrete specimen with 10% fly ash had the lowest corrosion rate value compared to other variations of fly ash concrete specimens. However, it had a lower value than the 100OPC and 100PPC concrete specimens.
3. The function of time greatly affected the increase in the diffusivity of chloride ions where in this study the time immersion affected the impedance value of the electrochemical impedance spectroscopy (EIS) fitting.
4. The limitation of this study is that the use of fly ash made from biomass from sawdust has limited by-products due to its economic value. Further work will focus on comparing it with fly ash made from Refused Derived Fuel (RDF) which contains chloride and analyse its effect on the strength of concrete.

REFERENCES

- [1] MESDM, "Electric Power Supply Business Plan (RUPTL 2019-2028)," 2019.
- [2] Ministry of State Secretariat, *Peraturan Pemerintah Nomor 22 Tahun 2021 tentang Pedoman Perlindungan dan Pengelolaan Lingkungan Hidup*, vol. 1, no. 078487A. 2021, p. 483.
- [3] U.S. EPA, "Environmental Protection Agency 40 CFR Parts 257 and 261 Hazardous and Solid Waste Management System; Disposal of Coal Combustion Residuals From Electric Utilities; Final Rule / Rules and Regulations," *Fed Regist*, vol. 80, no. 74, 2015.
- [4] I. Vázquez-Rowe, K. Ziegler-Rodriguez, J. Laso, I. Quispe, R. Aldaco, and R. Kahhat, "Production of cement in Peru: Understanding carbon-related environmental impacts and their policy implications," *Resour Conserv Recycl*, vol. 142, pp. 283–292, 2019, doi: 10.1016/j.resconrec.2018.12.017.
- [5] S. Uthaman, R. P. George, V. Vishwakarma, M. Harilal, and J. Philip, "Enhanced Seawater Corrosion Resistance of Reinforcement in Nanophase Modified Fly Ash Concrete," *Constr Build Mater*, vol. 221, pp. 232–243, 2019, doi: 10.1016/j.conbuildmat.2019.06.070.
- [6] R. Riastuti, A. Cahyadi, Y. Pratesa, and S. T. Siallagan, "The Study of Corrosion Resistance of Reinforcement Steel Embedded in Concrete Composed of Commercial Portland Cement and Final Tin Slag Against Chloride Environment," in *IOP Conference Series: Materials Science and Engineering*, Institute of Physics Publishing, 2018. doi: 10.1088/1757-899X/431/5/052006.
- [7] E. Bachtiar *et al.*, "Monitoring of chloride and Friedel's salt, hydration components, and porosity in high-performance concrete," *Case Studies in Construction Materials*, vol. 17, p. 22, 2022, doi: <https://doi.org/10.1016/j.cscm.2022.e01208>.
- [8] C. Gunasekara, D. Law, S. Bhuiyan, S. Setunge, and L. Ward, "Chloride Induced Corrosion in Different Fly Ash Based Geopolymer Concretes," *Constr Build Mater*, vol. 200, pp. 502–513, 2019, doi: 10.1016/j.conbuildmat.2018.12.168.
- [9] ASTM C136, *Standard Test Method for Sieve Analysis of Fine and Coarse Aggregates*. West Conshohocken, PA, USA: ASTM International, 2001.
- [10] ASTM C192, *Standard Practice for Making and Curing Concrete Test Specimens in the Laboratory*. West Conshohocken, PA, USA: ASTM International, 2018.
- [11] ASTM C39, *Standard Test Method for Compressive Strength of Cylindrical Concrete Specimens*. West Conshohocken, PA, USA: ASTM International, 2016.
- [12] ASTM C1754, *Standard Test Method for Density and Void Content of Hardened Pervious Concrete*. West Conshohocken, PA, USA: ASTM International, 2012.
- [13] ASTM C1585, *Standard Test Method for Measurement of Rate of Absorption of Water by Hydraulic-Cement Concretes*. West Conshohocken, PA, USA: ASTM International, 2007.
- [14] ASTM C618, *Standard Specification for Coal Fly Ash and Raw or Calcined Natural Pozzolan for Use in Concrete*. West Conshohocken, PA, USA: ASTM International, 2014.
- [15] B. H. Ortiz-Salcedo, J. M. Paris, C. C. Ferraro, R. Minkara, and K. A. Riding, "Evaluation of chlorides in fly ash for use in concrete," *Cleaner Materials*, vol. 5, p. 100098, 2022, doi: 10.1016/j.clema.2022.100098.
- [16] Y. Cui, L. Wang, J. Liu, R. Liu, and B. Pang, "Impact of particle size of fly ash on the early compressive strength of concrete: Experimental investigation and modelling," *Constr Build Mater*, vol. 323, no. January, p. 126444, 2022, doi: 10.1016/j.conbuildmat.2022.126444.
- [17] X. Wang *et al.*, "Effect of Fly Ash on The Self-Healing Capability of Cementitious Materials with Crystalline Admixture Under Different Conditions," *AIP Adv*, vol. 11, no. 7, 2021, doi: 10.1063/5.0056183.
- [18] P. Chindapasirt, W. Kroehong, N. Damrongwiriyapap, W. Suriyo, and C. Jaturapitakkul, "Mechanical Properties, Chloride Resistance and Microstructure of Portland Fly Ash Cement Concrete Containing High Volume Bagasse Ash," *Journal of Building Engineering*, vol. 31, p. 101415, 2020, doi: 10.1016/j.job.2020.101415.
- [19] A. Su, T. Chen, X. Gao, Q. Li, and L. Qin, "Effect of

- carbonation curing on durability of cement mortar incorporating carbonated fly ash subjected to Freeze-Thaw and sulfate attack,” *Constr Build Mater*, vol. 341, p. 127920, 2022, doi: 10.1016/j.conbuildmat.2022.127920.
- [20] J. Lizarazo-Marriaga, C. Higuera, I. Guzmán, and L. Fonseca, “Probabilistic Modeling to Predict Fly-Ash Concrete Corrosion Initiation,” *Journal of Building Engineering*, vol. 30, p. 101296, 2020, doi: 10.1016/j.jobe.2020.101296.
- [21] P. T. Bui, Y. Ogawa, and K. Kawai, “Long-Term Pozzolanic Reaction of Fly Ash in Hardened Cement-Based Paste Internally Activated by Natural Injection of Saturated Ca(OH)₂ Solution,” *Materials and Structures/Materiaux et Constructions*, vol. 51, no. 6, pp. 1–14, 2018, doi: 10.1617/s11527-018-1274-0.
- [22] F. Moghaddam, V. Sirivivatnanon, and K. Vessalas, “The effect of Fly Ash Fineness on Heat of Hydration, Microstructure, Flow and Compressive Strength of Blended Cement Pastes,” *Case Studies in Construction Materials*, vol. 10, pp. 1–13, 2019, doi: 10.1016/j.cscm.2019.e00218.
- [23] Y. Sun, K. Q. Wang, and H. S. Lee, “Prediction of compressive strength development for blended cement mortar considering fly ash fineness and replacement ratio,” *Constr Build Mater*, vol. 271, p. 121532, 2021, doi: 10.1016/j.conbuildmat.2020.121532.
- [24] Q. Zhou, C. Lu, W. Wang, S. Wei, C. Lu, and M. Hao, “Effect of fly ash and sustained uniaxial compressive loading on chloride diffusion in concrete,” *Journal of Building Engineering*, vol. 31, p. 101394, 2020, doi: 10.1016/j.jobe.2020.101394.
- [25] S. Kumar, P. Murthi, P. Awoyera, R. Gobinath, and S. Kumar, “Impact Resistance And Strength Development of Fly Ash Based Self-Compacting Concrete,” *Silicon*, 2020, doi: 10.1007/s12633-020-00842-2.
- [26] W. Nguyen, J. F. Duncan, T. M. Devine, and C. P. Ostertag, “Electrochemical Polarization and Impedance of Reinforced Concrete and Hybrid Fiber-Reinforced Concrete Under Cracked Matrix Conditions,” *Electrochim Acta*, vol. 271, pp. 319–336, 2018, doi: 10.1016/j.electacta.2018.03.134.
- [27] S. Mundra, M. Criado, S. A. Bernal, and J. L. Provis, “Chloride-induced corrosion of steel rebars in simulated pore solutions of alkali-activated concretes,” *Cem Concr Res*, vol. 100, pp. 385–397, 2017, doi: 10.1016/j.cemconres.2017.08.006.
- [28] J. K. Singh, S. Mandal, H. S. Lee, and H. M. Yang, “Effect of chloride ions concentrations to breakdown the passive film on rebar surface exposed to l-arginine containing pore solution,” *Materials*, vol. 14, no. 19, 2021, doi: 10.3390/ma14195693.
- [29] Y. Hoshi *et al.*, “Electrochemical Impedance Analysis of Corrosion of Reinforcing Bars in Concrete,” *Electrochemistry*, vol. 87, no. 1, pp. 78–83, 2019, doi: 10.5796/electrochemistry.18-00050.
- [30] W. Wei, Q. Liang, Z. Yu, and Z. Yong-sheng, “Electrochemical Impedance Spectroscopy Characteristics of Steel Corrosion in Seawater Sea- Sand Concrete,” in *IOP Conference Series: Earth and Environmental Science*, China: Institute of Physics Publishing, 2019, pp. 0–5. doi: 10.1088/1755-1315/267/4/042017.
- [31] S. H. Kang, Y. Jeong, M. O. Kim, and J. Moon, “Pozzolanic reaction on alkali-activated Class F fly ash for ambient condition curable structural materials,” *Constr Build Mater*, vol. 218, pp. 235–244, 2019, doi: 10.1016/j.conbuildmat.2019.05.129.
- [32] H. G. C. Silva, P. G. Terradillos, E. Zornoza, J. M. Mendoza-Rangel, P. Castro-Borges, and C. A. J. Alvarado, “Improving Sustainability Through Corrosion Resistance of Reinforced Concrete by Using a Manufactured Blended Cement and Fly Ash,” *Sustainability (Switzerland)*, vol. 10, no. 6, pp. 1–15, 2018, doi: 10.3390/su10062004.
- [33] B. C. & W. Green, *Corrosion and Protection of Reinforced Concrete*, 1st ed. London, UK: CRC Press, 2021.
- [34] O. A. Mohamed, “A review of Durability and Strength Characteristics of Alkali-Activated Slag Concrete,” *Materials*, vol. 12, no. 8, 2019, doi: 10.3390/ma12081198.
- [35] ASTM C876, *Standard test method for corrosion potentials of uncoated reinforcing steel in concrete*. West Conshohocken, PA, USA: ASTM International, 2015.